VNU Journal of Science: Mathematics - Physics
Journal homepage: https://js.vnu.edu.vn/MaP

Original Article

Study of Thermodynamic Properties and Melting Curves of HP2 Structure Thallium Metal Under Extreme Conditions

Nguyen Thi Hong*

Hong Duc Unniversity, 565 Quang Trung, Dong Ve, Thanh Hoa, Vietnam

Received 25th March 2025
Revised 27th April 2025; Accepted 10th June 2025

Abstract: Thermodynamic properties are important to understand and simulate thermodynamic processes, calculate and predict temperature, efficiency changes, improve energy efficiency in industrial systems. In this work, we studied the effect of pressure on several thermodynamic quantities including Debye frequency, Debye temperature, and Debye-Waller factor of HP2-structured Thallium (Tl) metal in which we considered the effect of non-ideal c/a axis ratio using a semi-empirical method. The correlation shift function in the X-ray absorption fine structure spectrum was determined on the basis of the Debye-Waller factor. The effective interaction potential between scattering and absorbing atoms with other neighboring atoms was approximately determined by the contribution of neighboring atoms to the fourth coordination sphere. Applying the Debye model, we obtain the volume (pressure) dependent analytical expressions of thermodynamic quantities including Debye frequency, Debye temperature, Debye - Waller factor. In addition, we have combined the Debye model and Lindemann melting law to determine the melting temperature of Tl metal. The previous experimental parameters are introduced by us to numerically calculate these thermodynamic quantities up to a pressure of 50 GPa. The melting curve of Tl according to our calculations is compared with compared with previous theoretical and experimental results and show good agreement. This study not only provides additional data on the thermodynamic properties of Tl metal but can also be applied to calculate other metals and alloys under extreme conditions.

Keywords: Thallium, Debye model, Debye frequency, Debye–Waller factor, high pressure, Lindemann's law of melting.

1. Introduction

The study of the physical properties of materials at high and ultrahigh pressures is an important research area. This topic is attracted the attention of many researchers in materials science, geophysics, planetary science and nuclear physics [1-23]. It can provide deeper insights into the chemistry as well

* Corresponding author.
E-mail address: nguyenthihongvatly@hdu.edu.vn

https//doi.org/10.25073/2588-1124/vnumap.4997

as the structure, properties and internal dynamics of large planets under extreme conditions. Experimentally, researchers today can measure various physical properties of materials at pressures up to hundreds of GPa [11, 20, 22]. The experimental results provide an important database for verifying and developing the equation of state, phase stability and melting in condensed matter physics. Therefore, theoretically, the prediction of thermodynamic properties as well as melting curves of materials at high pressures has become of topical and scientific significance.

Thallium is used in gamma ray detectors, in heavy liquids for mineral leaching, infrared photoresistors, high-index glasses, radio diagnostics in nuclear medicine, high-temperature superconductors for applications such as magnetic resonance imaging, magnetic energy storage, magnetic propulsion, power generation and transmission. Tl isotopes may be utilized as a monitor of the marine manganese oxide burial flux over million year time scales [3]. In addition, Thallium isotopes can be used to calculate the magnitude of hydrothermal fluid circulation through the oceanic crust [3]. Thallium has many applications but is a highly toxic metal even at low concentrations. Therefore, understanding the thermodynamic properties of these metals under environmental conditions and even under extreme conditions is necessary for the current problem of heavy metal pollution in soils in order to determine the level and find the cause of pollution, thereby proposing technological solutions as well as sustainable development strategies. To the best of our knowledge, there have been many research works carried out using different methods and approaches to study the thermodynamic properties, melting temperature of Thallium metal at different temperature and pressure conditions [20, 22-25]. In [20], from the electronic structure calculations based on first principles, density functional theory (DFT) and experimental studies, Kotmool et al. have shown the abnormal deformation in the structural phase of Thallium metal caused by high pressure. In some cases, the agreement between different experiments and theories is quite good, but in the high temperature and pressure region, the calculation results from the above studies do not agree well with the experiments, many experiments need to be matched because they have not reached the desired temperature and pressure conditions. The obtained values of thermodynamic quantities of Tl metal at high pressure between studies are still controversial, even contradictory [22, 25]. In particular, there are very few studies on the Debye-Waller factor (DWF), Debye frequency and temperature of these metals at high pressure. Or if there are studies, they are only in the case of ideal hcp crystals (i.e. the axis ratio $c/a=\sqrt{8/3}$) while in reality, solid crystals are often in the HP2 structure (the axis ratio $c/a\neq\sqrt{8/3}$) [26-27].

In the present work, some thermodynamic properties of Thallium metal with HP2 structure, considering the anisotropy (non-ideal c/a axis ratio) at high pressure will be studied by developing Anharmonic Correlated Debye Model (ACDM) combining the Lindemann melting criterion and Vinet equation of state. We perform numerical calculations for Thallium metal up to a pressure of 50 GPa. Our theoretical results will be compared with previous theoretical and experimental results to verify the developed theory.

2. Theoretical Approach

2.1. Thermodynamic Quantities in ADM

The Extended X-ray Absorption Fine Structure (EXAFS) provides information about the number of atoms in an atomic layer and its Fourier image provides information about the radius of the atomic layers {Formatting Citation}. From there, people have also built models to determine thermodynamic

parameters, thermal vibration effects and many other important physical effects of solids. Therefore, EXAFS has become a very useful method in analyzing and determining the structure of objects. At low temperatures, anharmonic effects can be ignored, but at high temperatures, these effects are significant and if the anharmonic contribution is not considered, we may get incorrect information about the object [29, 30]. To explain and determine the errors caused by anharmonic effects, many theoretical models have been built, in particular, classical anharmonic correlated Einstein model (CACE) has achieved remarkable results in studying EXAFS spectra including anharmonic components. However, CACE is based on the assumption that all atoms in the crystal oscillate with the same frequency, which does not include the dispersion expression. Recently, ACDM has been built on the perspective of the local oscillation picture with the correlated contributions of neighboring atoms, which takes into account the dispersion of phonons (atoms in the crystal oscillate with varying frequencies), ACDM has built an approximation of the cumulants expansion based on the following expression {Formatting Citation}.

$$\left\langle e^{2iqr} \right\rangle = \exp\left[2iqr_0 + \sum_{n=0}^{\infty} \frac{(2iq)^n}{n!} C^{(n)} \right],\ n = 1, 2, 3, \ldots \tag{1}$$

where r is the distance between two atoms at temperature T, r_0 is the distance between two atoms at equilibrium position, $C^{(n)}$ are the n-th order cumulants, in which, the second order cumulant $C^{(2)}$ describes the variance of the distance distribution, corresponding to the parallel mean square relative displacement, $C^{(2)}$ characterizes DWF or the damping coefficient of the EXAFS spectrum, Therefore, it is also referred to as DWF.

In this section, we develop ACDM to calculate for DWF, Debye frequency and temperature of pure metal of HP2 structure under the effect of high pressure, in which the atoms in the crystal lattice of the solid interact with each other, rather than being independent oscillators, The atoms in the solid are assumed to oscillate with frequency varying from 0 to the maximum value ω_D. The oscillations in the ACDM propagate with a constant sound velocity v_D in the crystal. The dispersion expression has a linear form $\omega = v_D.q$. The maximum frequency value is called the Debye frequency. The Debye temperature is defined as an important thermodynamic parameter characterizing the lattice oscillation of a solid that is related to the Debye by $\mathrm{h}\omega_D = k_B\theta_D$ (h is the reduced Planck constant, k_B is the Boltzmann constant). The value of the Debye temperature is usually determined from experimental measurements or through the determination of the elastic force constant.

In ACDM, the expression for the dispersion of light takes the form

$$\omega(q) = 2\sqrt{\frac{k_{eff}}{M}} \left| \sin\left(\frac{qa_h}{2} \right) \right|, \tag{2}$$

where, q is the wave number, $|q| \le \dfrac{\pi}{a_h}$, M is the total mass of the system, a_h is the lattice constant.

The Debye frequency and temperature are determined by the corresponding effective force constants k_{eff} as follows

$$\omega_D = 2\sqrt{\frac{k_{eff}}{M}},\ \theta_D = \frac{\mathrm{h}\omega_D}{k_B}. \tag{3}$$

The DWF of solids in ACDM was proposed by using the multi-particle system method that reported by N. V. Hung et al., when the number of atoms is large, the DWF is calculated by the corresponding integral as follows [32].

$$C_2 = \left\langle x^2 \right\rangle - \left\langle x \right\rangle^2 \approx \left\langle x^2 \right\rangle = -\frac{\mathrm{h}a_h}{2\pi}\frac{1}{k_{eff}}\int_0^{\pi/a_h} \omega(q)\frac{1+z(q)}{1-z(q)}dq, \tag{4}$$

where
$$z(q) = \exp\left(\beta \mathrm{h}\omega(q)\right),\ \beta = \frac{1}{k_B T}. \tag{5}$$

The relationship between the lattice constant and the volume of the crystal is given by

$$a_h = a_{0h}\left(V/V_0\right)^{1/3} = a_{0h}\left(\eta\right)^{1/3}, \tag{6}$$

where, a_{0h} is the value of the lattice constant at pressure $0\left(\mathrm{GPa}\right)$, $\eta = \frac{V}{V_0}$ is the crystal volume compression factor.

The pressure dependence of k_{eff} can be evaluated through the Debye frequency that can be indirectly determined by the Grüneisen parameter defined in the Debye model as follows

$$\gamma_G = -\frac{\partial \ln \omega_D}{\partial \ln V}. \tag{7}$$

Several hypotheses have been proposed to describe the volume dependence of the Grüneisen parameter [33-34]. In the paper, we apply the proposal of Burakovsky et al., for the effect of pressure on the Grüneisen parameter of materials as follows [6].

$$\gamma_G = \frac{1}{2} + \gamma_1 \eta^{1/3} + \gamma_2 \eta^s, \tag{8}$$

where γ_1, γ_2, $s > 1$ are the values depending on the studied material.

Performing mathematical transformations, we obtain the volume dependent expressions of the Debye frequency and temperature, respectively, as

$$\omega_D(\eta) = \omega_{0D}\eta^{-1/2}\exp\left[-3\gamma_1\left(\eta^{1/3}-1\right) - \frac{\gamma_2}{s}\left(\eta^s - 1\right)\right], \tag{9}$$

$$\theta_D(\eta) = \theta_{0D}\eta^{-1/2}\exp\left[-3\gamma_1\left(\eta^{1/3}-1\right) - \frac{\gamma_2}{s}\left(\eta^s - 1\right)\right], \tag{10}$$

where ω_{0D} and θ_{0D} are the Debye frequency and temperature at zero pressure, respectively. These quantities can be determined from experimental measurements or from ACDM as follows

$$\omega_{0D} = 2\sqrt{\frac{k_{eff}^0}{M}},\ \theta_{0D} = \frac{\mathrm{h}\omega_{0D}}{k_B}. \tag{11}$$

The effective force constant of the material at zero pressure k_{eff}^0 is calculated by us based on the anharmonic effective (AE) expression in ACDM.

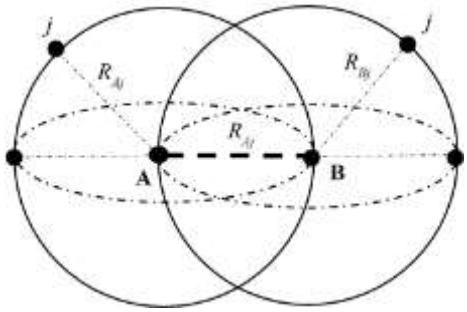

Figure 1. Absorber atom (A), back-scattered atom (B) and their first coordination spheres.

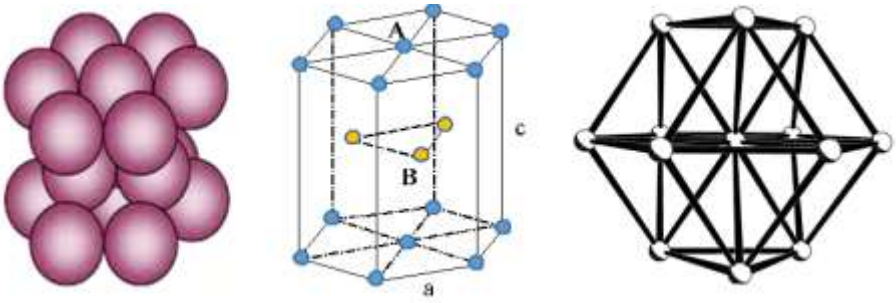

Figure 2. HP2 crystal structure.

The AE potential can better represent the interactions in systems where the atoms make large displacements, while the usual pair interaction only takes into account the harmonic approximation with small fluctuations around the equilibrium state. The AE potential can include the influence of temperature on the thermodynamic or structural properties of the material. Furthermore, instead of considering only the interactions of individual pairs of atoms, the anharmonic effective potential can incorporate contributions from many-to-many atom interactions, nonlinear interactions, phonon interactions, etc., which can significantly affect the behavior of complex multi-particle systems or systems that change phase or structure. The AE potential expression has the following form [35]

$$V_{eff}\left(x\right)=\varphi\left(x\right)+\sum_{j\neq i}^{i=A,B}\varphi\left(\frac{M_AM_B}{\left(M_A+M_B\right)M_i}x\hat{R}_{AB}\hat{R}_{\mathrm{ij}}\right)=\frac{1}{2}k_{0eff}x^2+k_3x^3+k_4x^4+...,\ x=r-r_0 \tag{12}$$

where r and r_0 are the nearest neighbor distances between two atoms, respectively, in the present investigation and equilibrium states; $\varphi\left(x\right)$ describes the interaction potential between the absorber atoms A (with the mass of M_A)) and back-scattered atoms B (with the mass of M_B); the main term $\sum_{j\neq i}^{i=A,B}\varphi\left(\frac{M_AM_B}{\left(M_A+M_B\right)M_i}x\hat{R}_{AB}\hat{R}_{\mathrm{ij}}\right)$ is the contribution of the nearest neighbor atoms to the oscillation of the absorber and back-scattered atoms; the sum j is over all their nearest neighbors; $\hat{R}_{AB}$ is the unit vector directed from the absorber atom to the back-scattered atom; $\hat{R}_{\mathrm{ij}}$ is the unit vector directed from the i-th atom to the j-th atom; k_{0eff} is the effective force constants; k_3 and k_4 are, respectively, the cubic and quartic anharmonic force constants due to the anharmonicity caused by thermal lattice vibrations.

We apply this assumption to calculate for a pure metal crystal of HP2 structure (Figure 2) with axial ratio $c/a = e$ (a and c are two lattice constants). By doing approximate calculations to the second coordination sphere, we obtain the expression of the effective interaction potential as follows

$$V_{eff}^{HP2}(x) = \varphi(x) + 4\varphi\left(\frac{-\sqrt{3}x}{2\left(3e^2+4\right)^{1/2}}\right) + 4\varphi\left(\frac{\sqrt{3}x}{2\left(3e^2+4\right)^{1/2}}\right) + 4\varphi\left(\frac{x\left(3e^2-2\right)}{2\left(4+3e^2\right)}\right) + 4\varphi\left(\frac{-x\left(2+3e^2\right)}{2\left(4+3e^2\right)}\right) + 2\varphi\left(\frac{x\left(4-3e^2\right)}{2\left(4+3e^2\right)}\right) \tag{13}$$

We assumed that the interaction potential between the absorber atom and the back-scattered atom with their neighboring atoms can be described by the Morse pair interaction potential. In the 4th order displacement approximation, this interaction potential takes the following form

$$V(x) = D_0\left[e^{-2\alpha x} - 2e^{-\alpha x}\right] \approx D_0\left(-1 + \alpha^2x^2 - \alpha^3x^3 + \frac{7}{12}\alpha^4x^4\right), \tag{14}$$

where parameter D_0 is the dissociation energy, α describes the width of the potential energy

Substituting expression (14) into equation (13), we obtain the expression for the effective interaction potential $V_{eff}(x)$ of the HP2 crystal structure as follows

$$V_{eff}^{HP2}(x) \approx -19D_0 + D_0\beta^2x^2\left(1 + \frac{6}{4+3e^2} + 4.\left(\frac{\left(3e^2-2\right)}{2\left(4+3e^2\right)}\right)^2 + 4.\left(\frac{\left(2+3e^2\right)}{2\left(4+3e^2\right)}\right)^2 + 2.\left(\frac{\left(4-3e^2\right)}{2\left(4+3e^2\right)}\right)^2\right)$$
$$- D_0\beta^3x^3\left(1 + 4.\left(\frac{\left(3e^2-2\right)}{2\left(4+3e^2\right)}\right)^3 + 4.\left(\frac{-\left(3e^2+2\right)}{2\left(4+3e^2\right)}\right)^3 + 2.\left(\frac{\left(4-3e^2\right)}{2\left(4+3e^2\right)}\right)^3\right) +$$
$$+ \frac{7}{12}D_0\beta^4x^4\left(1 + \frac{9}{2\left(4+3e^2\right)^2} + 4.\left(\frac{x\left(3e^2-2\right)}{2\left(4+3e^2\right)}\right)^4 + 4.\left(\frac{\left(2+3e^2\right)}{2\left(4+3e^2\right)}\right)^4 + 2.\left(\frac{\left(4-3e^2\right)}{2\left(4+3e^2\right)}\right)^4\right). \tag{15}$$

From equations (15) and (12) we determined the effective force constant k_{eff}^{HP2} according to the Morse potential parameters as

$$k_{eff}^{HP2} = 2D_0\beta^2.\left\{1 + \frac{6}{4+3e^2} + 4.\left(\frac{\left(3e^2-2\right)}{2\left(4+3e^2\right)}\right)^2 + 4.\left(\frac{\left(2+3e^2\right)}{2\left(4+3e^2\right)}\right)^2 + 2.\left(\frac{\left(4-3e^2\right)}{2\left(4+3e^2\right)}\right)^2\right\}. \tag{16}$$

2.2. Melting Temperature

In this section, we will present an approach to the problem of melting of materials at high pressure based on the combination of Lindemann melting condition and the Debye model. The Lindemann melting condition has been shown by Wang et al., [36] as the following formula.

$$T_m = const.V^{2/3}.\theta_D^2 . \tag{17}$$

where the crystal volume V and the Debye temperature θ_D are pressure-dependent quantities.

Performing mathematical transformations. we obtain an explicit analytical expression of the melting temperature T_m depending on the compressibility factor η as

$$T_m = T_0 \eta^{-1/3} \exp\left\{6\gamma_1\left(1-\eta^{1/3}\right)+\frac{2\gamma_2}{s}\left(1-\eta^{s}\right)\right\}, \tag{18}$$

where, T_0 is the melting temperature of the material under normal conditions.

2.3. Equation of State

To determine the influence of pressure on the thermodynamic quantities (Debye frequency and temperature, EXAFS DWF coefficient, and melting temperature) obtained in the previous section, we need to know the relation between pressure *P* and the compressibility coefficient η , or the equation of state (EOS) of the material. There are many EOS used to study the thermodynamic properties as well as the phase transition of materials at high pressure such as Birch-Murnaghan EOS [37], and Vinet EOS [38], In the work [39], Cohen et al., have shown that Vinet EOS gives the most accurate results of the pressure-volume-temperature relationship at high pressure. Therefore, in this thesis, we will use Vinet equation to evaluate the influence of pressure on the thermodynamic properties of materials. Vinet EOS is constructed in the following form [38].

$$P = 3K_0\eta^{-2/3}\left(1-\eta^{1/3}\right)\exp\left[\frac{3}{2}\left(K_0^{'}-1\right)\left(1-\eta^{1/3}\right)\right], \tag{19}$$

where, K_0, $K_0^{'}$ are the isothermal bulk compressibility moduli and their first derivatives with respect to pressure, respectively. These values can be determined by experimental measurements or DFT simulations.

3. Results and Discussion

In this section, to discuss the effectiveness of the present theoretical model in calculating and analyzing the pressure-dependent EXAFS oscillations of Tl metal, we use the expressions obtained from Section 2, in which the Morse potential parameters, the Grüneisen parameters, the isothermal bulk modulus and its first derivative with respect to pressure Tl metal are taken from experimental corresponding as $\alpha = 1,23608\left(\text{Å}^{-1}\right)$, $D_0 = 0,35888\left(eV\right)$, $r_0 = 3.5609\left(\text{Å}\right)$[40, 41], $\gamma_1 = 1.39$, $\gamma_2 = 0.54$, $s = 7.3$ and $T_0 = 577$, $K_0 = 42\left(\text{GPa}\right)$, $K_0^{'} = 6,5$ [6]. Several studies have shown that at ambient pressure and temperature, the crystal structure of Tl is hexagonal packed and this structure remains unchanged up to 68 GPa [26]. In this work, we calculate the pressure dependence of thermodynamic quantities of Tl up to a pressure of 50 GPa. One fact that needs to be considered is that the compression of the hcp structure is anisotropic. In particular, the c-axis is less compressed than the a-axis, so that the c/a ratio increases with increasing pressure, which was pointed out by Cazola et al., in {Formatting Citation}. This work also shows that the c/a ratio increases from 1.596 at ambient pressure to 1.610 at 3.4 GPa and tends to increase at higher pressures. Applying the theoretical model given in Part 2, we calculate the effective force constant, Debye frequency and temperature at zero

pressure and ambient temperature of Tl with values measured of $a = 3.4568$ and $c = 5.5259$ [11], respectively as shown in Table 1.

Table 1. Thermodynamic quantities obtained at zero pressure and ambient temperature of Tl and experimental Debye temperature value of Tl metal

Metal	k_{eff} (eV/Å^2)	ω_D $(\times 10^{13}$ Hz$)$	θ_D (K)	$\theta_D^{\exp}$ (K)*
Tl	2.74165	2.27687	85.7697	88 [24]; 88, 78.5 [42]; 76.5 [43]

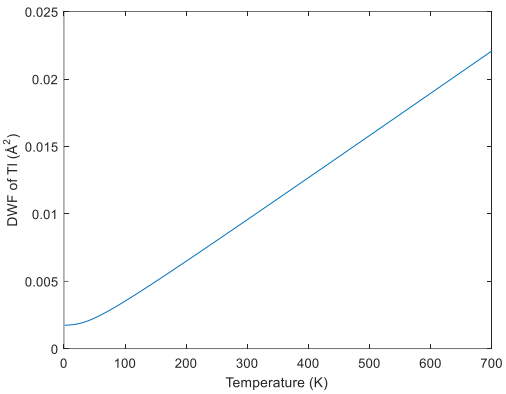

Figure 3. Debye – Waller factor of Tl metal under the effect of temperature with non-ideal axial ratio *c*/*a*.

In Fig. 3, we show the temperature dependence of DWF of Tl metal. The results show that DWF of Tl metal increases with temperature, specifically, at temperature $2\,\mathrm{K}$, DWF has a value of $1{,}746.\ 10^{-3}\left(\text{Å}^2\right)$, at temperature $700\,\mathrm{K}$, DWF has a value of about $2{,}216.10^{-2}\ \left(\text{Å}^2\right)$. This increase can be explained based on the nature of crystal lattice oscillations that as the temperature increases, the oscillations energy of the atoms in the crystal lattice also increases, the average displacement from the equilibrium position increases. This leads to an increase in the DWF. In the low temperature range (below $100\,\mathrm{K}$), DWF increases slowly (on the graph it has a gentle parabolic shape), in the higher temperature range, DWF increases almost linearly with increasing pressure. This shows the significant effect of the enharmonic factor on crystal lattice oscillations in the high temperature region.

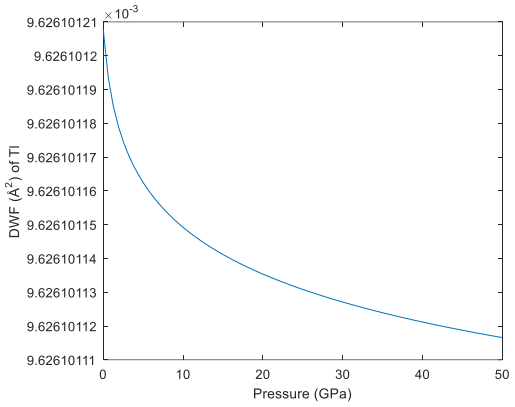

Figure 4. Pressure-dependent DWF of Tl metal with non-ideal axial ratio *c*/*a*.

The pressure dependence of DWF of Tl metal at ambient temperature is shown in Fig. 4. The calculation results show that DWF of Tl metal decreases with increasing pressure. At pressure $0\left(\mathrm{GPa}\right)$, the value of DWF of Tlq is about $9.6261.10^{-3}\left(\mathrm{\AA}^2\right)$. This decrease in DWF can be explained by the limited oscillations of atoms with increasing pressure, leading to a decrease in the mean square relative displacement between two intermediate atoms. The results in Fig. 3 lead to the fact that although the change in DWF with pressure is not very large in absolute value, the clear decreasing trend shows that the effect of pressure on atomic oscillations is significant.

In Fig. 5, we show the pressure dependence of the Debye frequency of the Tl. The graph shows that the Debye frequency increases rapidly as the pressure increases. Specifically, when the pressure increases from $0\left(\mathrm{GPa}\right)$ to $50\left(\mathrm{GPa}\right)$, the Debye frequency increases from about $1.1225.10^{13}\left(\mathrm{Hz}\right)$ to $3.2504.10^{13}\left(\mathrm{Hz}\right)$. This result can be explained that when the pressure increases, the atoms in the crystal lattice are compressed, reducing the inter-atomic distance. According to the theory of crystal lattice oscillations, when the distance between atoms decreases, the restoring force increases, leading to an increase in the oscillations frequency of the atoms. The increase in the Debye frequency has shown that pressure significantly affects the stiffness of the crystal lattice.

In Fig. 6, we show the pressure dependence of the Debye temperature of the metal Tl to $50\left(\mathrm{GPa}\right)$. In the pressure range below $10\left(\mathrm{GPa}\right)$, the graph shows that the Debye temperature increases almost linearly with pressure, but at higher pressure ranges $10\left(\mathrm{GPa}\right)$ the slope of the graph gradually decreases. To the best of our knowledge, there are currently no experimental studies on the DWF, Debye temperature or Debye frequency of Tl in the high-pressure range, however, our results may provide further data on the thermodynamic properties of Tl at high pressure as well as serve as reference data for future theoretical and experimental studies.

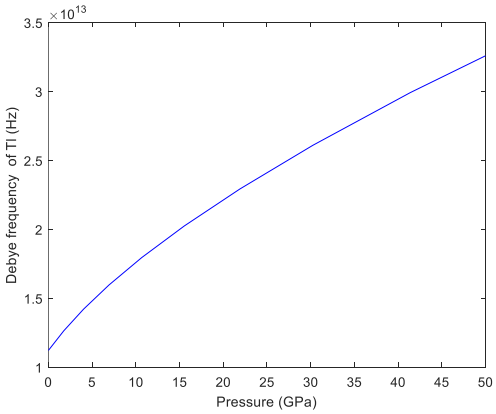

Figure 5. Pressure-dependent frequency of Tl metal with non-ideal axial ratio *c*/*a*.

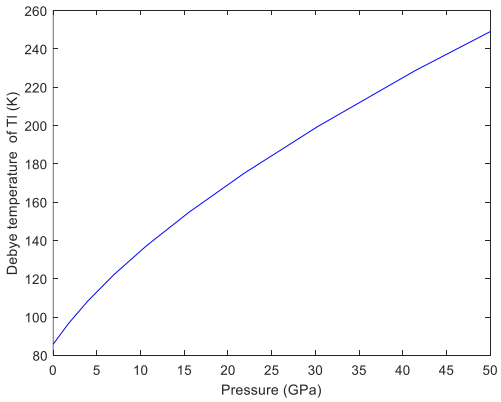

Figure 6. Debye temperature of Tl under the effect pressure.

In Fig. 7, we present our calculation results on c/a ratio-dependent DWF of Tl. From this figure, we can see that DWF decrease rapidly almost linearly with increasing c/a ratio. c/a ratio-dependent Debye frequency and temperature of Tl metal at zero pressure is shown in Figs. 8 and 9. From these two figures we can see that the Debye frequency and temperature of Tl metal increase with the increase of the c/a axis ratio.

Comparing the results of pressure dependence with the dependence of the c/a axis ratio of thermodynamic quantities of Tl including DWF, Debye frequency, Debye temperature in Figs. 4-6 and Figs. 7-9, we see that the effect of pressure on thermodynamic quantities is greater than the effect of the c/a axis ratio. DWF decreases with pressure and also decreases with c/a ratio, Debye frequency and temperature increase with pressure and also increase with c/a ratio. This result can be explained the experiment of Cazola 2016 in [27] that the c/a ratio increases slightly with pressure.

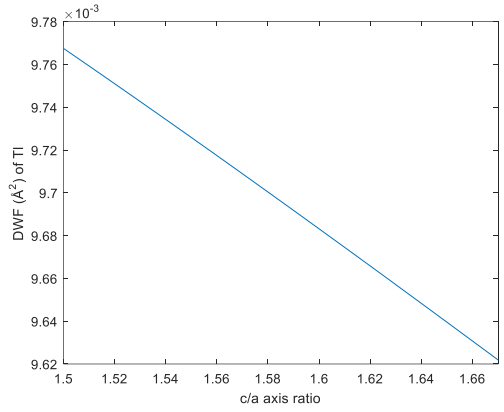

Figure 7. c/a ratio-dependent Debye–Waller factors of Tl.

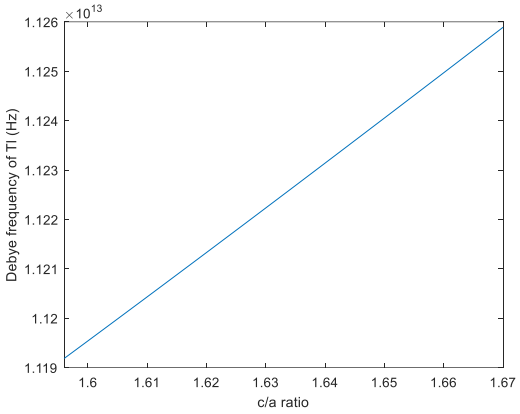

Figure 8. c/a ratio-dependent Debye frequency of Tl.

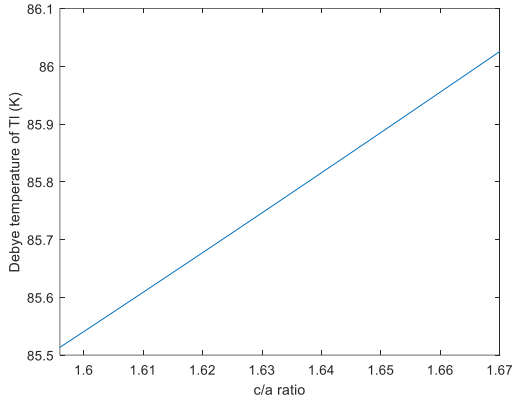

Figure 9. *c*/*a* ratio-dependent Debye temperature of Tl.

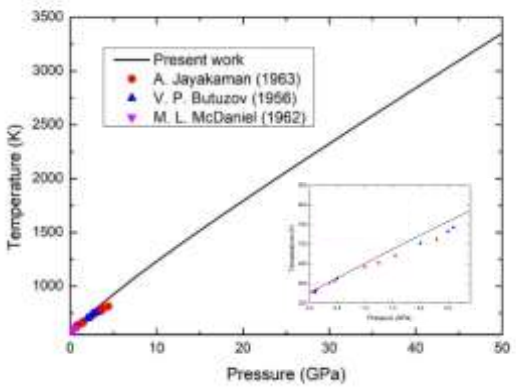

Figure 10. Melting curve of Tl under the effect of pressure.

The melting temperature curve of Tl metal under the effect of pressure (solid line) is shown in Fig. 10. Previous experimental data [22, 25] have also been included for comparison. The results in Fig. 10 show that the melting temperature of Tl increases rapidly and almost linearly with pressure. This can be explained that as the pressure increases, the bonding force between atoms increases, making the material more difficult to melt. The experimental data included in the graph for comparison show that our melting temperature curve agrees well with the experimental points of previous works. The difference between our results and the experimental values given for comparison is in the range of 0,25% to about 6%. The reason for the above difference may be that in the high-pressure region, our calculations are limited by

the approximation limit. However, the difference from the experiment is not high, this result can contribute significantly to the database of melting temperature of Tl metal under high pressure conditions.

4. Conclusion

In this work, we have studied the effect of pressure on thermodynamic quantities including Debye frequency and temperature, DWF and melting temperature of HP2-structured Tl metal by applying ACDM combined with modified Lindemann melting law. The calculation results indicate that DWF decrease gradually with pressure, frequency and Debye temperature increase gradually with pressure. This has shown the fact that the thermal oscillations of atoms in the Tl crystal lattice are limited at high pressure, at the same time, the change of c/a axis ratio also has a significant effect on the crystal lattice vibrations as well as thermodynamic quantities. The melting temperature of Tl increases almost linearly with pressure which can be explained that as the pressure increases, the binding force between atoms increases significantly. Our numerical calculation results are in quite good agreement with the collected experimental values which allows us to believe that the theory we have proposed can be extended to some other metals and alloys.

Reference

[1] L. Vočadlo, D. Alfè, G. D. Price, M. J. Gillan, Ab Initio Melting Curve of Copper by the Phase Coexistence Approach, J. Chem. Phys., Vol. 120, No. 6, 2004, pp. 2872-2878, https://doi.org/ 10.1063/1.1640344.

[2] S. Japel, B. Schwager, R. Boehler, M. Ross, Melting of Copper and Nickel at High Pressure: The Role of Electrons, Phys. Rev. Lett., Vol. 95, No. 16, 2005, pp. 1-4, https://doi.org/10.1103/PhysRevLett.95.167801.

[3] S. G. Nielsen, M. Rehkämper, J. Prytulak, Investigation and Application of Thallium Isotope Fractionation, Rev. Mineral. Geochemistry, Vol. 82, 2017, pp. 18, https://doi.org/10.2138/rmg.2017.82.18.

[4] N. V. Hung, T. S. Tien, N. B. Duc, D. Q. Vuong, High-order Expand XAFS Debye Waller Factors HCP Crystala Based on Classical Anharmonic Correlated Einstein Model, Vol. 28, No. 21, 2014, pp. 1450174, https://doi.org/10.1142/S0217984914501747.

[5] C. J. Wu, P. Söderlind, J. N. Glosli, J. E. Klepeis, Shear-induced Anisotropic Plastic Flow from Body-Centred-Cubic Tantalum before Melting, Nature Materials, Vol. 8, No. 3, 2009, pp. 223-228, https://doi.org/ 10.1038/nmat2375.

[6] L. Burakovsky, L. Preston, Analytic Model of the Grüneisen Parameter all Densities, J. Phys. Chem. Solids, Vol. 65, No. 8-9, 2004, pp. 1581-1587, https://doi.org/10.1016/j.jpcs.2003.10.076.

[7] A. B. Belonoshko et al., Molybdenum at High Pressure and Temperature: Melting from Another Solid Phase, Physical Review Letters, Vol. 100, No. 13. 2008, https://doi.org/10.1103/PhysRevLett.100.135701.

[8] T. D. Cuong, N. Q. Hoc, N. D. Trung, N. T. Thao, D. P. Anh, Theoretical Predictions of Melting Behaviors of hcp Iron up to 4000 GPa, Phys. Rev. B, Vol. 106, 2022, pp. 094103, https://doi.org/10.1103/PhysRevB.106.094103.

[9] M. Ross, R. Boehler, D. Errandonea, Melting of Transition Metals at High Pressure and The Influence of Liquid Frustration: The Late Metals Cu, Ni, and Fe, Physical Review B - Condensed Matter and Materials Physics, Vol. 76, No. 18. 2007, https://doi.org/ 10.1103/PhysRevB.76.184117.

[10] T. S. Tien, Analysis of Temperature-dependent Extended X-ray Absorption Fine Structure Oscillation of Distorted Crystalline Cadmium, Commun. Phys., Vol. 32, No. 4, 2022, pp. 401-412, https://doi.org/10.15625/0868-3166/16890.

[11] J. S. Olsen, L. Gerward, S. Steenstrup, E. Johnson, A High-Pressure Study of Thallium, J. Appl. Crystals, Vol. 27, No. 6, 1994, pp. 1002-1005, https://doi.org/10.1107/S002188989400720X.

[12] B. P. Grad, R. B. Moore, EXAFS Studies of Various Sulfonated and Carboxylated Cadmium Ionomers, Am. Chem. Soc., Vol. 29, 1996, pp. 1685-1690, https://doi.org/10.1021/ma951058e.

[13] Y. Fujinaga, Y. Syono, The Cadmium-zinc Phase Diagram Under High Pressure, High Pressure Research, High Press. Res., Vol. 15, No. 4, 1997, pp. 233-243, https://doi.org/10.1080/08957959708244244.

[14] I. F. Vasconcelos, E. A. Haack, P. A. Maurice, A. B. Bunker, EXAFS Analysis of Cadmium(II) Adsorption to Kaolinite Igor, Chem. Geol., Vol. 249, 2008, pp. 237-249, https://doi.org/10.1016/j.chemgeo.2008.01.001.

[15] M. A. Marcus, W. Flood, M. Stiegerwald, L. Brus, M. Bawendi, Structure of Capped CdSe Clusters by EXAFS, Journal of Physical Chemistry, Vol. 95, No. 4. 1991, pp. 1572–1576, https://doi.org/10.1021/j100157a012.

[16] A. Carter, C. Bouldin, Surface Structure of Cadmium Selenide Nanocrystallites, Physical Review B-Condensed Matter and Materials Physics, Vol. 55, No. 20. 1997, pp. 13822-13828, https://doi.org/10.1103/PhysRevB.55.13822.

[17] B. K. Godwal, S. V. Raju, Z. Geballe, R. Jeanloz, Electronic Phase Transitions in Cadmium at High Pressures, J. Phys. Conf. Ser., Vol. 337, 2012, pp. 012033, https://doi.org/10.1088/1742-6596/377/1/012033.

[18] P. G. P. S. Kulsum et al., A State of the Art Review on Cadmium Uptake, Toxicity and Tolerance in Rice: from Physiological Response to Remediation Process, Environ. Res., Vol. 220, 2023, pp. 115098, https://doi.org/10.1016/j.envres.2022.115098.

[19] R. M. Alshegaihi et al., Effective Citric Acid and EDTA Treatments in Cadmium Stress Tolerance in Pepper (Capsicum annuum L.) Seedlings by Regulating Specific Gene Expression, South African J. Bot., Vol. 159, 2023, pp. 367-380, https://doi.org/10.1016/j.sajb.2023.06.024.

[20] K. Kotmool et al., High Pressure Induced Distortion in Face Centered Cubic Phase of Thallium, Proc. Natl. Acad. Sci., Vol. 113, No. 40, 2016, pp. 11143-11147, https://doi.org/10.1073/pnas.1612468113.

[21] P. D. Pathak, R. J. Desai, Thermal Properties of Some HCP Metals, Physica Status Solidi (a), Vol. 62, No. 2, 1980, pp. 625-629, https://doi.org/10.1002/pssa.2210620234.

[22] M. L. McDaniel, S. E. Babb, G. J. Scott, Melting Curves of Five Metals under High Pressure, J. Chem. Phys., Vol. 37, No. 4, 1962, pp. 822-828, https://doi.org/10.1063/1.1733167.

[23] J. F. Cannon, Behavior of the Elements at High Pressures, J. Phys. Chern. Ref. Data, Vol. 3, 1974, pp. 781-824, https://doi.org/10.1063/1.3253148.

[24] P. Endla, X-Ray Determination of Debye Temperature and Microhardness of Some HCP Elements Re, Os and Tl, IOP Conf. Ser. Mater. Sci. Eng., Vol. 1119, 2021, pp. 012001, https://doi.org/10.1088/1757-899X/1119/1/012001.

[25] A. Jayaraman, W. Klement, R. C. Newton, G. C. Kennedy, Fusion Curves and Polymorphic Transitions of the Group III Elements-Aluminum, Gallium, Indium and Thallium-at High Pressures, J. Phys. Chem. Solids, Vol. 24, No. 1, 1963, pp. 7-18, https://doi.org/10.1016/0022-3697(63)90036-2.

[26] O. Schulte, W. B. Holzapfel, Effect of Pressure on the Atomic Volume of Ga and Tl up to 68 GPa, Physical Review B - Condensed Matter and Materials Physics, Vol. 55, No. 13. 1997, pp. 8122-8128, https://doi.org/10.1103/PhysRevB.55.8122.

[27] C. Cazorla, S. G. MacLeod, D. Errandonea, K. A. Munro, M. I. McMahon, and C. Popescu, Thallium Under Extreme Compression, J. Phys. Condens. Matter, Vol. 28, No. 44, 2016, pp. 445401, https://doi.org/10.1088/0953-8984/28/44/445401.

[28] N. V. Hung, R. Frahm, Hi. Kamitsubo, Anharmonic Contributions to High Temperature EXAFS Spectra Theory and Comparison with Experiment, J. Phys. Soc. Jpn., Vol. 65, 1996, pp. 3571, https://doi.org/10.1143/JPSJ.65.3571.

[29] A. V. Poiarkova, J. J. Rehr, Multiple Scattering X-ray Absorption Fine Structure Debye-Waller Factor Calculations, Physical Review B - Condensed Matter and Materials Physics, Vol. 59, No. 2, 1999, pp. 948-957, https://doi.org/10.1103/PhysRevB.59.948.

[30] E. A. Stern, P. Livṇ, Z. Zhang, Thermal Vibration and Melting From a Local Perspective, Physical Review B, Vol. 43, No. 11, 1991, pp. 8850-8860, https://doi.org/10.1103/PhysRevB.43.8850.

[31] G. Bunker, Application of the Ratio Method of EXAFS Analysis to Disordered Systems, Nucl. Instruments Methods Phys. Res., Vol. 207, No. 3, 1983, pp. 437-444, https://doi.org/10.1016/0167-5087(83)90655-5.

[32] N. V. Hung, N. B.o Trung, B. Kirchner, Anharmonic Correlated Debye Model Debye-Waller Factors, Phys. B Condens. Matter, Vol. 405, No. 11, 2010, pp. 2519-2525, https://doi.org/10.1016/j.physb.2010.03.013.

[33] J. C. Graf, M. J. Greeff, C. K. Boettger, High-Pressure Debye-Waller and Grüneisen Parameters of Gold and Copper, Vol. 65, 2004, pp. 65-68, https://doi.org/10.1063/1.1780185.

[34] H. K. Hieu, Melting of Solids Under High Pressure, Vacuum, Vol. 109, 2014, pp. 184-186, https://doi.org/10.1016/j.vacuum.2014.07.010.

[35] N. V. Hung, J. Rehr, Anharmonic Correlated Einstein Model Debye-Waller Factors, Phys. Rev. B - Condens. Matter Mater. Phys., Vol. 56, No. 1, 1997, pp. 43-46, https://doi.org/10.1103/PhysRevB.56.43.

[36] Y. Wang, R. Ahuja, B. Johansson, Melting of Iron and Other Metals at Earth's Core Conditions: A Simplified Computational Approach, Phys. Rev. B - Condens. Matter Mater. Phys., Vol. 65, No. 1, 2001, pp. 1-3, https://doi.org/10.1103/PhysRevB.65.014104.

[37] N. Tsujino, Y. Nishihara, Y. Nakajima, E. Takahashi, K. Funakoshi, Y. Higo, Equation of State of γ-Fe: Reference Density for Planetary Cores, Earth Planet. Sci. Lett., Vol. 375, 2013, pp. 244-253, https://doi.org/10.1016/j.epsl.2013.05.040.

[38] P. Vinet, J. Ferrante, J. H. Rose, J. R. Smith, Compressibility of solids, J. Geophys. Res. Geophys Res, Vol. 92, No. B9, 1987, pp. 9319-9325, https://doi.org/10.1029/JB092iB09p09319.

[39] R. E. Cohen, O. Gülseren, R. J. Hemley, Accuracy of Equation of State Formulations, Am. Mineral., Vol. 85, No. 2, 2000, pp. 338-344, https://doi.org/10.2138/am-2000-2-312.

[40] G. Singh, R. P. S. Rathore, Generalised Morse Potential for BCC Complex Metals, Vol.135, No. 2, 1986, pp. 513-518, https://doi.org/10.1002/pssb.2221350208.

[41] N V. Hung, T. S. Tien, L. H. Hung, R. R. Frahm, Anharmonic Effective Potential, Local Force Constant and EXAFS of Crystial: Theory and Comparison to Experiment, Int. J. Mod. Phys. B, Vol. 22, No. 29, 2008, pp. 5155–5156, https://doi.org/10.1142/S0217979208049285.

[42] E. Purushotham, N.G. Krishna, Mean Square Amplitudes of Vibration and Associated Debye Temperatures of Rhenium, Osmium and Thallium, Phys. B., Vol. 405, 2010, pp. 3308-3311, https://doi.org/10.1016/j.physb.2010.04.066.

[43] B. D. Singh, Y. P. Varshni, X-ray Debye Temperature for Hexagonal Crystals, Acta Cryst, Vol. 38, 1982, pp. 854-858, https://doi.org/10.1107/S0567739482001740.